*Reprinted from*
*"Research in Heat Transfer"*
PERGAMON PRESS
OXFORD · LONDON · NEW YORK · PARIS
1963

*Printed by Adlard & Son Ltd., Dorking, Surrey, England*

# Recent Studies on Quantitative Spectroscopy and Gas Emissivities*

S. S. PENNER,† D. B. OLFE,‡ and M. LAPP§

Daniel and Florence Guggenheim Jet Propulsion Center
California Institute of Technology
Pasadena, California

Representative theoretical and experimental studies relating to the determination of gaseous radiation from isothermal systems are discussed. The following recently concluded studies are described: *f*-number measurements for OH behind shock fronts; a method for the direct determination of radiative and collisional life times of vibrationally excited, molecules; emissivity calculations for $CO_2$; emissivity calculations for a hydrogen plasma at temperatures up to about 10,000°K.

## I. INTRODUCTION

The physical basis of thermal radiation has been well understood since the advent of modern quantum theory. A fairly detailed account of the apparatus required for the calculation of gas emissivities from spectroscopic data has been described in a recently published text.[1] We refer to this book for justification and appropriate reference sources concerning the basic relations which we shall use in the following discussion.

Of primary significance in theoretical calculations of equilibrium gas emissivities are absolute intensities (or *f*-numbers) for all of the transitions that make measurable contributions to the observed radiant energy output. Experimental methods that have been used successfully in the past for the determination of these basic physical constants are described, for example, in ref. 1. Recent attempts in our laboratory to use less widely recognized procedures for absolute intensity determinations are outlined in section II.

Once the basic spectroscopic parameters have been defined, it is a simple matter to calculate spectral and total emissivities, albeit through the use of a formidable analytical apparatus.[1] In section III we present a summary of recent computations on $CO_2$ and on a hydrogen plasma.

Procedures for performing radiative transfer calculations have been

* The work described in this report has been supported, in part, by the Office of Naval Research, U.S. Navy, under Contract Nonr-220(03), NR 015 401 and, in part, by the Office of Scientific Research, U.S. Air Force, under Contract AF 18(603)-2. This paper has been prepared for presentation at an ASME Heat Transfer Symposium in New York City, November 1960.

† Professor of Jet Propulsion, California Institute of Technology, Pasadena, California.
‡ Now Associate Professor of Aeronautics, New York University, New York City, N.Y.
§ Now staff member, General Electric Research Laboratory, Schenectady, N.Y.

well worked out for non-isothermal systems but require detailed knowledge of spectral absorption coefficients. For excellent accounts of these calculations we refer to CHANDRASEKHAR[2] and KOURGANOFF.[3] Unfortunately, it is practically impossible to specify reasonable values for the spectral absorption coefficients in most of the radiating systems encountered in engineering practice. For this reason, practical applications often involve the use of "effective average absorption coefficients". A better method of approach should, however, be possible. We have described previously a procedure[4, 5] for utilizing available emissivity data[6] in radiative transfer calculations for non-isothermal molecular emitters. Although it is apparent that the use of total emissivity data is effectively restricted to pure gases with overlapped spectral lines, and cannot be extended to gas mixtures without careful allowance for overlapping bands and lines (i.e. without performing essentially a classical transfer calculation of the type formulated by CHANDRASEKHAR[2] and KOURGANOFF[3]), the method should serve at least as an illustration of a useful procedure for non-isothermal emitters.

## II. ABSOLUTE INTENSITY MEASUREMENTS

Useful procedures for the experimental determination of absolute intensities for gases are described, for example, in chapter 6 of ref. 1. In the following discussion we shall restrict ourselves to an outline of an absolute intensity measurement for OH behind a reflected shock wave (section IIA) and to the description of some considerations relating to the direct determination of vibrational life times for molecular emitters.

### A. Absolute intensity measurements for OH behind reflected shocks*

Although absolute intensity or *f*-number determinations using the shock tube have been described by several experimenters,[8] it is quite difficult to develop a definitive procedure with acceptable accuracy. The problems encountered in experimental studies of this type will now be described by considering a recently concluded study for a vibration–rotation band belonging to the $^2\Sigma \rightarrow {}^2\Pi$ transitions of OH.[7] Earlier measurements for these bands have been performed by a number of investigators using other methods.[9–11]

The emission of OH was observed as a function of time in the axial direction behind the reflected shock wave. The experimental conditions were chosen in such a way that no OH emission could be detected from the gas behind the incident shock wave. The radiation was monitored with a 1P28 photomultiplier used in conjunction with a Perkin–Elmer monochromator. We found that the emitted intensity was a linear function of time after a short induction period, thus indicating that the radiating region was transparent.

* This section is abstracted from ref.7.

In order to determine the $f$-number, an absolute intensity calibration was made by imaging a source of known intensity at the shock tube exit port. All tests were performed with $H_2O$–Ar mixtures containing about 1 per cent of $H_2O$.

Conventional shock-tube techniques were used in order to define the shock velocity, (theoretical) gas temperature, and equilibrium gas composition. The overall response time of the photomultiplier circuitry used for obtaining time-resolved data was less than 0·45 μsec. Theoretical calculations of shock-tube performance were carried out at the Rand Corporation with an IBM 704 program developed by R.E. Duff of Los Alamos.

(1) *Relaxation time for OH formation.* A representative oscilloscope trace is shown in Fig. 1 for a measured incident shock velocity of 1·27 mm/μsec.

The shape of the curve shown in Fig. 1 may be understood by referring

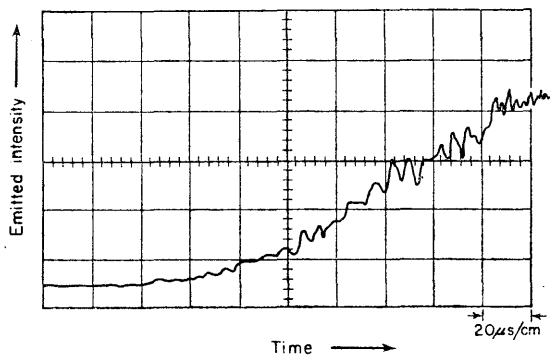


FIG. 1. *Single-beam oscilloscope trace* (1·15 *per cent* $H_2O$, $p_1 \simeq 50{\cdot}3$ *mm* Hg, $u_s \simeq 1{\cdot}27$ *mm/μsec) for the emitted intensity belonging to lines of the* (0, 0)*—band,* $^2\Sigma \rightarrow {}^2\Pi$ *transitions, of* OH.

to the schematic diagram shown in Fig. 2. The gas at $x=x'$ has been in the state characteristic of region 5 for a time $t'=(L-x')/u_{sr}$ where $u_{sr}$ is the reflected shock velocity. The partial pressure of OH at $x'$ is $p_5^*(t')$. If we let $R_{\bar{\lambda}}^{\circ}$ =the average blackbody radiancy and $\alpha$=the integrated intensity of the observed transitions, then we obtain for the steradiancy (in erg/sec-cm$^2$-steradian)

$$B=\frac{1}{\pi}R_{\bar{\lambda}}^{\circ}\alpha\int_0^L p_5^*(t')\mathrm{d}x'=\frac{1}{\pi}R_{\bar{\lambda}}^{\circ}\alpha p_5^*\int_0^L f_0\left(\frac{L-x'}{u_{sr}}\right)\mathrm{d}x' \qquad (1)$$

where $p_5^*(t')=p_5^* f_0(t')$, $p_5^*$ is the value of the OH partial pressure at chemical equilibrium, $f_0(0)=0$ and $\lim_{t\to\infty} f_0(t)=1'$. An appropriate form for $f_0(t')$ is $1-\exp(-t'/\tau)$ where $\tau$ is an effective time constant for the reaction. Hence

$$\frac{B}{\frac{1}{\pi}R_{\lambda}^{\circ}\ \alpha p_5}=\int_0^L\left[1-\exp\left(-\frac{L-x'}{\tau u_{sr}}\right)\right]dx'=L-\tau u_{sr}\left[1-\exp^{-L/\tau u_{sr}}\right]$$

But $L=u_{sr}t$ whence it follows that

$$B=\frac{1}{\pi}R_{\lambda}^{\circ}\alpha p_5 u_{sr}\left[t-\tau(1-e^{-t/\tau})\right] \tag{2}$$

and

$$B\simeq\frac{1}{\pi}R_{\lambda}^{\circ}\ \alpha p_5\begin{cases}\times u_{sr}(t-\tau) & \text{for } t\gg\tau\\ \times u_{sr}(\tau/e) & \text{for } t=\tau\\ \times u_{sp}(t^2/2\tau) & \text{for } t\ll\tau\end{cases}$$

Equation. (2) provides an acceptable fit to the experimental data shown in Fig. 1 for a suitably chosen value of $\tau$. Our estimated values of $\tau$ were found to

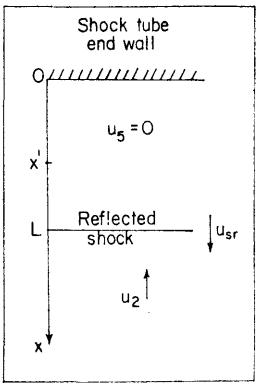


FIG. 2. *Reflected shock coordinates.*

agree within about 20 per cent with values derived from previously published kinetic studies.[12]

(2) *Absolute intensity measurements.* The following measurements are required for an absolute intensity determination:

(*a*) the fraction of the total intensity to which the spectrograph-detector combination responds;

(*b*) the absolute intensity of the source radiancy that is actually recorded by the detector;

(*c*) the instrumental output as a function of the absolute incident energy flux.

A schematic diagram of the optical system used for intensity calibrations and for converting observed intensities to absolute intensities is shown in

Fig. 3. If we let $R_T$ represent the total radiant flux (erg/sec) produced by heated OH, then

$$R_T \simeq \frac{1}{\pi}\left[\begin{array}{c}\text{source radiancy } R_s \\ \text{(erg/cm}^2\text{-sec-A-2}\pi \\ \text{sterad)}\end{array}\right] \times \left[\left[\begin{array}{c}\text{source solid angle} \\ \triangle\Omega_s \text{ subtended} \\ \text{by the source} \\ \text{optics (sterad)}\end{array}\right] \times \left[\begin{array}{c}\text{source} \\ \text{area} \\ A\triangle_s \\ \text{(cm}^2\text{)}\end{array}\right] \times \left[\begin{array}{c}\text{wavelength} \\ \text{interval} \\ \triangle\lambda\text{(A)}\end{array}\right]\right] \times \left[\begin{array}{l}\text{intensity loss factor } F \text{ produced} \\ \text{by quartz optics, off-axis rays,} \\ \text{and a ratio smaller than 1 of} \\ \text{the shock tube exit port area} \\ \text{to the area of the image made of} \\ \text{the source}\end{array}\right] \times \left[\begin{array}{l}\text{ratio } Y \text{ of the intensity} \\ \text{from the shock tube in} \\ \text{mv per mv of the cali-} \\ \text{bration intensity cor-} \\ \text{responding to } R_s\end{array}\right] \quad (3)$$

The quantity $R_T$ is related to $B$ as follows:

$R_T = B \times$ (solid angle subtended by the receiver optical system)
$\times$ (shock-tube exit area actually viewed).

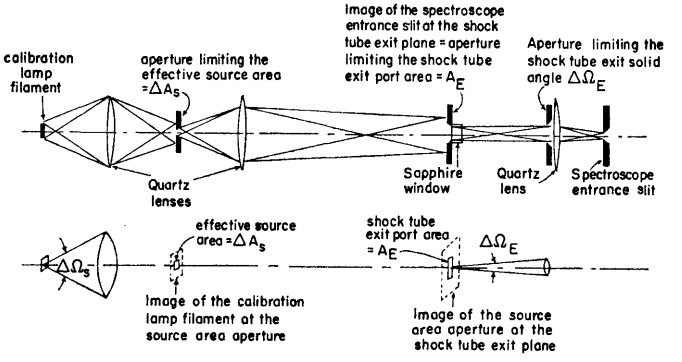


FIG. 3. *Schematic diagram of the optical system used for intensity calibrations and for converting observed intensities to absolute intensities.*

The effect of the instrumental slit function on Eq. (3) must also be considered. The experimentally determined slit function[13]* $g(|\lambda - \lambda_0|; b')$ is shown in Fig. 4 together with representative calculated[14] relative intensities of lines belonging to the $^2\sum \rightarrow {}^2\Pi$ transitions of OH. The other factors required in Eq. (3) were obtained[7] by careful examination of the optical system and/or direct calibration studies. Absolute calibrations were performed with a tungsten lamp with a known surface emissivity operated at a known temperature.

* The value of $g$ determines the fraction of the available intensity at $\lambda$ to which the system responds when set at $\lambda_0$.

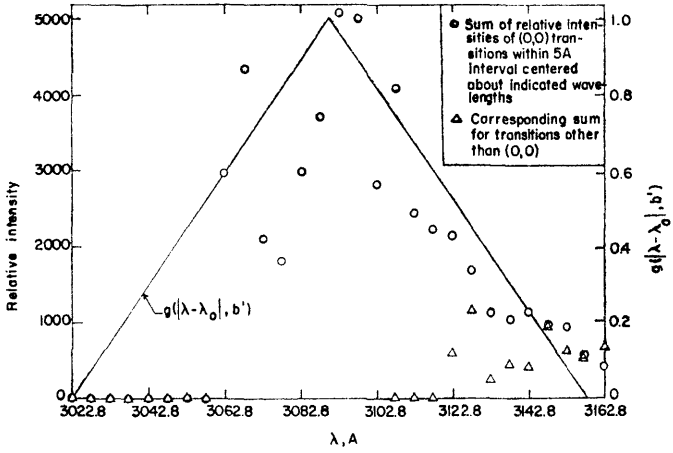


FIG. 4. *Relative intensities of* $OH\ ^2\Sigma \rightarrow {}^2\Pi$ *transitions at* 3000°*K over a selected portion of the spectrum.*[14] *Intensities lying between* 0 *and* 30 *on the scale used for the ordinate are indicated as* 0. *The spectroscopic slit function* $g(|\lambda - \lambda_0|;b')$ *is also shown.*

The integrated intensity $\alpha = \underset{(0,0)\text{-band}}{f} P_\lambda d\lambda$ is related to the $f$-number through the expression

$$\alpha_{(0,0)} \simeq \frac{\pi e^2}{mc^2} \frac{N_l}{p} \lambda_0^2 f \simeq 0{\cdot}0227 \left(\frac{273}{T}\right) f \text{ atm}^{-1} \tag{4}$$

where $\lambda_0 = 3090$ A, $p =$ pressure in atm and $N_l =$ number of molecules per unit volume in the ground state $\simeq$ total number of molecules per unit volume. The $f$-number defined by Eq. (4) is the total $f$-number for the (0, 0) - vibrational band of the $^2\Sigma \rightarrow {}^2\Pi$ transitions of OH.

Since the OH radiators are in the linear part of the curves of growth, we may use Eq. (2) to relate the partial integrated intensity $\alpha'$ of the OH transitions that make contributions falling within the limits of the slit function to the experimentally measured radiant flux $R_T$. Thus

$$R_T = B\triangle\Omega_E A_E = \frac{1}{\pi} R_\lambda^\circ \triangle\Omega_E A_E \alpha' p_5^* u_{rs} (t - \tau) \tag{5}$$

In order to allow for the slit function in Eq. (5), we must use for $\alpha'$ the expression

$$\alpha' = \Sigma\, g(|\lambda - \lambda_0|, b') S_J$$

all OH transitions for which the slit function is non-zero,
where $S_J$ is the integrated intensity of the $J$th line. For the measured triangular slit function* and $\lambda_0 = 3090$ A, we find

* Inaccuracies in the measurement of the slit function do not materially alter this result since most of the intensity is concentrated near the center of the slit function.

$$G \equiv \frac{\Sigma \quad g(|\lambda-\lambda_0|, b')S_J}{\Sigma \quad S_J} = 0{\cdot}67$$

all OH transitions for which the slit function is non-zero

all (0, 0)-band transitions

from tabulated[14] relative intensities (compare Fig. 4). The correct value of the integrated intensity ($\alpha_{(0,0)}$) of the (0, 0)-band is then given by

$$\alpha_{(0,0)} = \alpha'/G = \alpha'/0{\cdot}67 \tag{6}$$

Using appropriate numerical values, we obtain

$$f = (0{\cdot}90 \pm 0{\cdot}10) \times 10^{-3} \tag{7}$$

for the (0, 0)-band, $^2\Sigma \rightarrow {}^2\Pi$ transitions of OH. The indicated 10 per cent uncertainty represents the root mean square scatter of the shock-tube data.

Previously published values for the $f$-number are $1{\cdot}0 \times 10^{-3}$ (OLDENBERG and RIEKE[9]), $0{\cdot}5 \times 10^{-3}$ (DYNE[10]) and $\simeq 1{\cdot}3 \times 10^{-3}$ (CARRINGTON[11]) after correcting to equivalent thermodynamic data for the computation of the partial pressures of OH. Oldenberg and Rieke and Dyne produced OH radicals by heating $H_2O$–$O_2$ mixtures in furnaces to about 1400–1500°K. Densitometer records of photographic absorption spectra were used to provide the absorption coefficient profiles ($P_\omega$) of selected lines. The line integrated intensities ($S$) were obtained through use of the relation $S_{\text{line}} = \int_{\text{line}} P_\omega d\omega$ and were then corrected by extrapolation to "zero intensity". Carrington's measurements were carried out with various $H_2$–$O_2$ and propane–$O_2$ flames. The $f$-number was measured by the "curve-of-growth" method.

An overall estimate of the experimental accuracy in our experiments is about $\pm 60$ per cent, i.e. $f = (0{\cdot}9 \pm 0{\cdot}5) \times 10^{-3}$ although it is difficult to give an exact figure because of uncertainties in the temperature $T_5$. About half of this error estimate arises from uncertainties in the state functions, intensity calibration procedures, and shock-tube data, and half arises from quantities associated with the calibration source and with the definition of the shock-tube exit optics.

Several (possibly partially compensating) effects tend to make $T_5$ somewhat uncertain:

(1) Reflected shock velocities $u_{sr}$ and pressures in Ar lower than those calculated from the usual gas dynamic relations have been observed experimentally[15, 16] and predicted theoretically.[17] These lower reflected shock velocities correspond to lower temperatures $T_5$.

(2) The OH formed immediately behind the reflected shock is initially at a higher temperature than the calculated equilibrium value of $T_5$.

(3) It is possible that excessive populations of OH in the $^2\sum$ state may be produced behind shock fronts as is known to occur in flames. This problem can be settled only by performing a difficult, time-resolved population temperature measurement for the OH radicals formed behind a shock wave. We note that the first effect tends to make our computed *f*-number too small while the second and third effects tend to make it too large. A rough estimate of the first effect based on experimental data[15, 16] and on Goldsworthy's theoretical relations[17] indicates an *f*-number increase of perhaps 20–40 per cent.

### B. Measurements of radiative and collisional transition probabilities for molecular emitters in cylindrical chambers containing isothermal, dilute mixtures*

The emitted radiation intensity from a molecular system is proportional to the number of molecules in the excited state from which emission occurs. We consider vibrational excitation in the presence of an external radiation field and de-excitation in the absence of the field for stationary, dilute systems in cylindrical containers in which surface deactivation of excited species is so effective as to reduce the concentration of vibrationally excited molecules to zero at the bounding surfaces. The mathematical problem is similar to that encountered in the study of isothermal explosion limits with catalytic surfaces.[19] We presume that the maximum fraction of vibrationally excited molecules is sufficiently small to permit the approximation that the system remains isothermal at the temperature $T$ and at constant pressure $p$ and density $\rho$. In the following analysis we examine the rate of excitation in an external radiation field and the subsequent rate of de-excitation when the external radiation field is removed. The external radiation field is assumed to be of such high intensity, compared with thermal radiation in the system, that the latter may be considered to be negligibly small. Internal reflection and scattering are not allowed for explicitly; however, occurrence of reflection and scattering will not invalidate our radiative life time measurement.

Since we deal with isothermal and constant pressure systems at constant composition, the integrated energy, momentum and continuity equations are satisfied automatically. Only the species conservation equations with zero mass average velocity need to be considered. Furthermore, we restrict our considerations to pure gases (e.g. CO, $CO_2$, NO, etc.) and small number densities of vibrationally excited molecules. Hence only the continuity equation for the molecules in the first excited vibrational level needs to be considered. Using a binary mixture approximation, we find[20] that

$$\frac{\partial n_1}{\partial t} - D\nabla^2 n_1 = -\dot{w}_1 + \dot{w}_2 \tag{8}$$

where $n_1$ represents the number of molecules per cm$^3$ in the first vibrationally

* This section is abstracted from ref. 18.

excited level, $t$ denotes the time, $D$ is the binary diffusion coefficient for diffusion of vibrationally excited molecules through molecules in the ground state, $\nabla^2$ denotes the Laplacian operator, $-\dot{w}_1$ is the rate of removal of vibrationally excited molecules by gas-phase collisions and radiative transitions, and $\dot{w}_2$ is the rate of production of vibrationally excited molecules in the presence of an external radiation field. We must now specify the functional forms of $\dot{w}_1$ and of $\dot{w}_2$.

(1) *Excitation in an external radiation field.* The sum of the rates of de-excitation $-\dot{w}_1$ and of excitation $\dot{w}_2$ consists of contributions made by gas-phase collisions and by radiative transitions. RUBIN and SHULER[21] have noted that the collisional transitions, to the LANDAU–TELLER[22] approximation, obey the same selection rules as radiative transitions, viz. collisional energy exchange occurs only between adjacent vibrational levels.

The mathematical problem for the rate of excitation in an external radiation field may[18] then be reduced, in the harmonic oscillator approximation, to the solution of the problem specified below:

$$\left.\begin{aligned} &\frac{\partial n_1}{\partial t} - D\nabla^2 n_1 = -\gamma n_1 + \dot{w}_2 \\ &\gamma = (A_{1\to 0} + k_{1\to 0}) \\ &\dot{w}_2 = (A_{1\to 0}e^{-\theta'} + k_{1\to 0}e^{-0})n_T \end{aligned}\right\} \tag{9}$$

the boundary conditions are

$$n_1(t, x_l \text{ at the wall}) = 0$$

and

$$n_1(0, x_l) \simeq 0$$

if the steady-state concentration of $n_1$ is unobservably small prior to illumination. Here $A_{1\to 0}$ is the Einstein coefficient for spontaneous emission of radiation from the first excited vibrational level to the ground level; $k_{1\to 0} = \eta Z_c$ is the collisional transition probability if $Z_c$ is the mean collision frequency of excited molecules in the gas phase and $\eta$ represents the collision efficiency (i.e. the probability of de-excitation on collision); $\theta = h\nu_{1\to 0}/kT$ represents the reduced vibrational temperature if $\nu_{1\to 0}$ is the characteristic normal vibration frequency, $h$ denotes Planck's constant, and $k$ is the Boltzmann constant; $\theta' = h\nu_{1\to 0}/kT'$ if $T'$ is the effective blackbody temperature for the external radiation field; $n_T$ denotes the total number of molecules per unit volume and $n0 \simeq n_T$.

In terms of the reduced variables

$$\left.\begin{aligned} &t' = t/\tau \\ &\tau = L^2/D, \text{ and} \\ &x'_l = x_l/L \end{aligned}\right\} \tag{10}$$

we find

$$\left.\begin{aligned} &\frac{\partial n_1}{\partial t'}-\nabla^2 n_1=-\tau\gamma n_1+\tau\dot{w}_2 \\ &n_1(t', x_l' \text{ at the wall})=0,\ n_1(0, x_l')=0 \end{aligned}\right\} \tag{11}$$

Here $L$ denotes a characteristic chamber length. For an infinite cylinder of radius $L$, the solution of the boundary-value problem specified in Eq. (11) takes the form

$$n_1(t', x_l')=n_1(t', r')=\tau\dot{w}_2 \sum_j \frac{1-e^{-(\tau\gamma+\omega)_j t'}}{\tau\gamma+\omega_j} \frac{\sqrt{2}}{J_1(\sqrt{\omega_j})} J_0(\sqrt{\omega_j} r') \frac{\sqrt{2}}{\sqrt{\omega_j}} \tag{12}$$

where $J_1$ and $J_0$ are Bessel functions of order 1 and 0, respectively. Furthermore, the total concetration of $n_1$ per unit length of cylinder becomes

$$\iiint_{V_l} n_1(t, r)\mathrm{d}V=2\pi L^2 \int_0^1 n_1(t', r')r'\mathrm{d}r'$$

whence

$$n_1^{T,l}(t')\equiv \iiint_{V_l} n_1(t, r)\mathrm{d}V=\tau\dot{w}_2 4\pi L^2 \sum_j \frac{1-e^{-(\tau\gamma+\omega)_j t'}}{(\tau\gamma+\omega_j)\omega_j}$$

where the boundary condition specified in Eq. (11) shows that

$$J_0(\sqrt{\omega_j})=0, \text{ i.e. } \omega_j=(J_{0_j})^2 \tag{13}$$

if $J_{0_j}$ denotes the roots of

$$J_0(x)=0$$

The steady-state value of $n_1^{T,l}(t')$ is evidently

$$n_{1,s.s.}^{T,l}=\tau\dot{w}_2 4\pi L^2 \sum_j \frac{1}{J_{0_j}^2(\tau\gamma+J_{0_j}^2)} \tag{14}$$

whence

$$\frac{n_1^{T,l}(t')}{n_{1,s.s.}^{T,l}}=\frac{\sum_j \dfrac{1-e^{-(\tau\gamma+J_{oj}2)t'}}{J_{0_j}^2(\tau\gamma+J_{0_j}^2)}}{\sum_j \dfrac{1}{J_{0_j}^2(\tau\gamma+J_{0_j}^2)}} \tag{15}$$

Reference to Eq. (15) shows that the excitation process is dominated by the term

$$e^{-\tau\gamma t'}=\exp-(A_{1\to 0}+k_{1\to 0})t$$

i.e. by the time constant

$$t_{exc}\sim \frac{1}{A_{1\to 0}+k_{1\to 0}}$$

On the other hand, $n_{1,s.s.}^{T,l}$ is directly proportional to $\tau$. In other words, the characteristic diffusion time $L^2/D$ must not be too small since, otherwise, wall de-excitation reduces the prevailing steady-state concentration. Thus an experimental measurement of the rate of excitation cannot be performed at too low pressures.

(2) *Relaxation after the light source is turned off.* After the steady-state has been reached and the external light source has been turned off, the primary process is that of de-excitation and the term $\dot{w}_2$ in Eq. (8) disappears. Furthermore, $n_1(0, x_l')=[n_1(t', r')]_{s.s.}$ where the steady-state value is determined from Eq. (12). For an infinite cylinder we find now that

$$\frac{n_1^{T,l}(t')}{n_{1,s.s.}^{T,l}} = \frac{\sum_j \frac{e^{-(\tau\gamma+J_{0j}^2)t'}}{J_{0j}^2(\tau\gamma+J_{0j}^2)}}{\sum_j \frac{1}{J_{0j}^2(\tau\gamma+J_{0j}^2)}} \tag{16}$$

(3) *Representative Calculations.* The infinite sums appearing in the equations for the number densities may be evaluated approximately either for very small or for very large values of $\tau\gamma$.

In order to obtain upper limits for the radiant energy output, we confine our attention to the case in which wall de-excitation is unimportant. Eq. (14) for the steady-state number of molecules per unit length of cylinder in the ground level becomes now

$$\frac{Cn_{1,s.s.}^{T,l}}{n_T} = 0{\cdot}7\pi L^2\, C \frac{(A_{1\to0}e^{-\theta'}+k_{1\to0}e^{-\theta})}{A_{1\to0}+k_{1\to0}} \tag{17}$$

where $C$ is the length of the cylindrical chamber. For CO we have[23] $A_{1\to0}=33$ sec$^{-1}$ and $\nu_{1,0}=2143$ cm$^{-1}$. At a temperature of 300°K, we find from the kinetic theory and from sound dispersion experiments[24, 25] that $k_{1\to0}=\eta Z_c\cong(10^{-4})\,(5\times10^9 p)$ sec$^{-1}$ and $D\simeq10^{-2}p^{-1}$ cm$^2$/sec where $p$ is the pressure in atmospheres. Thus, in order to satisfy the assumption that wall de-excitation is unimportant, we must have

$$\frac{L^2}{D}(A_{1\to0}+k_{1\to0})=\frac{L^2}{10^{-2p-1}}\,(33+5\times10^5 p)\gg J_{0j}^2\cong5$$

which yields $p\gg10^{-4}$ atm for a characteristic length of about 1·5 cm. Setting $p=10^{-3}$atm, we find that

$$k_{1\to0}=5\times10^2 \text{ sec}^{-1}$$

Since collisional de-excitation is of dominant importance for the relaxation processes, it is apparent that currently available infrared detectors (time constants$\simeq10^{-6}$ sec) possess sufficiently high time resolution for observation of the decay period.

We must now compute the magnitude of the emitted radiation in order to

determine whether detection with available infrared cells is, in fact, possible. The maximum intensity of radiation, $I_{max}$, reaching the detector will be

$$I_{max}=BCn_{1,s.s.}^{T,l}\ A_{1\to 0}h\nu_{1,\,0}$$

where $B$ is the fraction of the total emitted radiation reaching the detector, and includes collimation, lens and geometrical losses. With the use of Eq. (17), $I_{max}$ becomes

$$I_{max}=0{\cdot}7\pi L^2Cn_T\frac{A_{1\to 0}e^{-\theta'}+k_{1\to 0}e^{-\theta}}{A_{1\to 0}+k_{1\to 0}}h\nu_{1,\,0}B\,A_{1\to 0}$$

whence for CO with $T'=900°K$, $B=0{\cdot}1$, $CL^2=10$ cm$^3$, and $p=10^{-3}$ atm,

$$I_{max}\cong 2\times 10^{-6}\text{ watt.}$$

The NEP (noise-equivalent power) of a detector is defined as the incident power required on a detector to generate a signal equal to its rms noise level in a 1 c/s band width. For larger band widths, the NEP increases linearly with the square root of the band width.[26] In the wavelength region of interest, a typical modern detector will possess an NEP of about $10^{-10}$ watt. Considering a 10 kc band-pass as suitable for adequate time resolution in a CO relaxation measurement, and allowing a factor of 10 in excess of the detector noise level as a minimum for unequivocal observation, a signal level of about $10^{-7}$ watts should be detectable. Since this estimate is smaller by a factor of 10 than the calculated signal level, it appears that an experimental measurement of relaxation time is feasible from a study of the rate of decay of infrared radiation.

## III. EMISSIVITY CALCULATIONS

The theoretical calculation of equilibrium gas emissivities forms the contents of chapters 11, 12, 14, and 15 in ref. 1. Two extensions of the earlier work will now be described, viz. emissivity calculations for $CO_2$ (section IIIA) and for a hydrogen plasma at moderate temperatures (section IIIB).

### A. Emissivity calculations for $CO_2$*

It has been shown previously that the measured equilibrium emissivities for carbon dioxide at room temperature are consistent with the results derived from approximate computations using a "box approximation" or a "just-overlapping line model" for the vibration–rotation bands and the best available spectroscopic data for the fundamental vibration–rotation bands.[28] A recomputation[27] of the relevant data is shown in Fig. 5. More recently, Plass has performed machine calculations[29] for the spectral equilibrium emissivities of carbon dioxide and has obtained numerical data that are in good accord with direct experimental measurements at temperatures up to 600°K; however, the calculated values become relatively too small as the temperature is raised and significant discrepancies (of about a factor of 2–4) have been noted at temperatures between 1200°K and 2000°K.[30, 31] Pre-

* This section is abstracted from ref. 27.

sumably Plass did not obtain exact agreement with the experimental data at elevated temperatures because of lack of knowledge concerning the following basic information that is required in *a priori* emissivity computations: (1) absolute intensity estimates for harmonic bands and for combination bands at elevated temperatures and (2) the complex temperature dependence of spec-

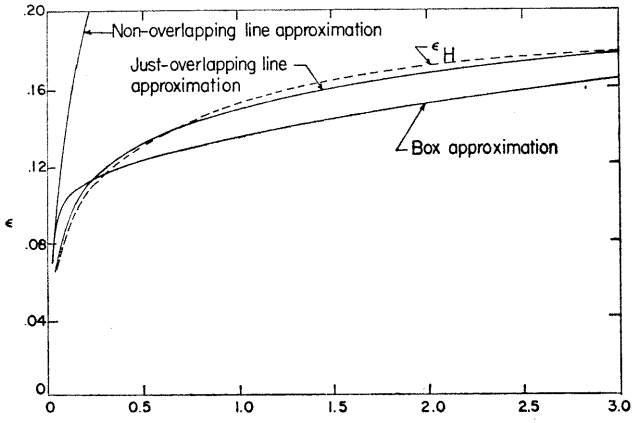


FIG. 5. *Emissivity calculations for carbon dioxide at* 300°*K, compared with the experimentally determined values* $\varepsilon_H$ *of Hottel.*

tral line shapes. In the following sections we describe a simple and useful procedure for total emissivity calculations that is relatively insensitive to possible errors in intensity and line profile descriptions.

(1) *Spectral, region and total emissivities.* Application of the Mayer–Goody procedure[32] to randomly distributed bands[33] shows that the mean value $\bar{\varepsilon}$ of the spectral emissivity at the wave-number $\omega$ is given by the relation

$$\bar{\varepsilon}_\omega = 1 - \exp(-\bar{A}/\delta^*_B) \tag{18}$$

where

$$\bar{A} = \int_0^\infty \mathscr{P}(\bar{\alpha}, \alpha)\, d\alpha \int_{-\infty}^{\infty} [1 - \exp(-P_{\omega'} X)]\, d\omega' \tag{19}$$

is the weighted-mean value of the band absorption

$$A = \int_{-\infty}^{\infty} [1 - \exp(-P_{\omega'} X)]\, d\omega'$$

which depends explicitly on the assumed band structure; $P_{\omega'}$ ($cm^{-1}$-$atm^{-1}$) is the spectral absorption coefficient at $\omega'$ for a uniformly distributed gas of optical depth $X$ (cm-atm) and the infinite integral in the defining relation for $A$ arises because we integrate between wave number limits that are arbitrarily larger and smaller than the wave number under consideration; the quantity

$\mathscr{P}(\bar{\alpha}, \alpha)d\alpha$ is the probability that a given band has an integrated intensity $\alpha$ ($cm^{-2}$-$atm^{-1}$) between $\alpha$ and $\alpha+d\alpha$ and $\bar{\alpha}$ is the mean integrated intensity of the randomly distributed vibration-rotation bands;* the quantity $\delta^*_B$ represents the mean band spacing. Equations (18) and (19) are applicable at $\omega$ if a large number $N$ of bands (i.e. more than about 5) with mean spacing $\delta^*_B$ contributes to $\bar{\varepsilon}_\omega$ and no contributions are made to $\bar{\varepsilon}_\omega$ by bands located outside of the interval $\omega \pm (N\delta^*_B/2)$.

Contributions to the emissivity of $CO_2$ are made by the vibration-rotation bands in 4 distinct spectral regions. If the $j$th region contains $N_j$ bands, then the weighted-mean value of the band absorption is computed from the relation

$$\bar{A}_j = \frac{1}{N_j} \left[ \sum_{i=1}^{N_j} A_i \right] \quad \text{evaluated for the bands in the } j\text{th spectral region} \tag{20}$$

In order to obtain the total emissivity $\varepsilon_j$ for the $j$th spectral region, we employ an average blackbody radiancy $R^o_{\bar{\omega}_j}$ and an effective region width $\triangle\omega_j$, i.e.

$$\varepsilon_j = \frac{R^o_{\bar{\omega}_j}}{\sigma T^4} (\bar{\varepsilon}_{\bar{\omega}_j}) \quad \triangle\omega_j = \frac{0{\cdot}3148}{T} \rho_j \bar{\varepsilon}_{\bar{\omega}_j} \triangle\omega_j \tag{21}$$

Here $\rho_j$ is the normalized blackbody function weighted with respect to the band absorptivities, viz.

$$\rho_j = \left[ \frac{\sum_i \rho_{\omega_i} A_i}{\sum_i A_i} \right] \quad \text{evaluated for bands in the } j\text{th region} \tag{22}$$

Using Eqs. (18), (20), and (21), we obtain the following formal representation for $\varepsilon_j$:

$$\varepsilon_j = \frac{0{\cdot}3148}{T} \rho_j \left\{ 1 - \exp\left[ - \frac{1}{\triangle\omega_j} \left( \sum_{i=1}^{N_j} A_i \right) \right] \right\} \triangle\omega_j \tag{23}$$

where $N_j = \triangle\omega_j/\delta^*_{B,j}$ is the number of contributing bands in the $j$th spectral region. Finally, the total emissivity $\varepsilon$ is calculated from the relation

$$\varepsilon = \sum_{\substack{\text{all contributing} \\ \text{spectral regions}}} \varepsilon_j \tag{24}$$

(2) *Emissivity calculations at* 600°K. The quantities $A_i$ and $\omega_i$ may be computed by using tabulated spectroscopic data. From the basic data we find also the region widths $\triangle\omega_j$.[27] The average distance $\delta^*_{B,j}$ between band centers has

* It is well known that the numerical value of $\bar{\varepsilon}(\omega)$ is practically independent of the precise form of $\mathscr{P}(\bar{a}, a)$ and that nearly equivalent results are obtained, for example, for an exponential distribution function and for equally intense bands.[32]

been set equal to the arithmetic average of the spacing between adjacent bands and the number of contributing bands $N_j$ becomes then the ratio $\triangle\omega_j/\delta^*_{B,j}$. Thus all of the spectroscopic data required for the computation of region and total emissivities are available.

Emissivities calculated [27] from Eqs. (23) and (24) for the just-overlapping band model are shown in Fig. 6 together with HOTTEL's[6] results. The observed satisfactory agreement between emissivities computed from spectroscopic data and the observed emissivities suggests that the model we have

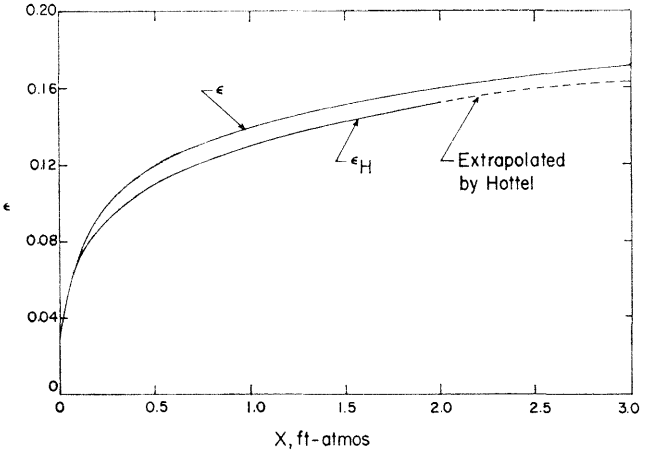


FIG. 6. *Comparison of calculated values of* $\varepsilon$ *with* $\varepsilon_H$ *at* 600°*K*.

adopted for calculation constitutes a reasonably satisfactory approximation.

The calculated emissivities for the spectral region containing the very strong $\nu_2$–fundamental of $CO_2$ have been found[27] to agree closely with results derived by Plass through the use of machine computations.

### B. Emissivity calculations for a hydrogen plasma at temperatures up to 10,000°K*

Radiant-heat transfer from a hydrogen plasma is of considerable interest in a number of engineering applications, e.g. power plants utilizing hydrogen as a driving fluid. For these applications it is necessary to consider pressures up to several hundred atmospheres and temperatures from several hundred °K to many thousands of °K. Accordingly, the emission for temperatures between 300°K and 10,000°K at high and low pressures has been considered (see ref. 35 for a calculation of the continuous emission above 10,000°K). Above 10,000°K, the emissivity will be essentially unity for high pressures and moderate or large mean beam lengths [cf. Fig. 7 and ref. 35].

Only equilibrium radiation from a pure hydrogen plasma was considered. However, this work may be adapted easily to the case where other constituents are present.

* This section is abstracted from ref. 34.

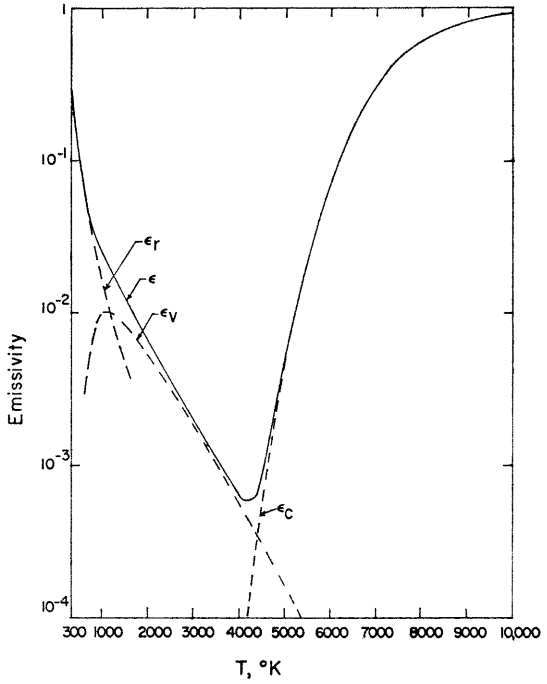


FIG. 7. *The total emissivity* $\varepsilon$ *of a hydrogen plasma for* $p_T=100$ *atm and* $l=30$ *cm. The dashed lines indicate emissivity contributions from the pressure-induced rotational lines* ($\varepsilon_r$) *and fundamental band* ($\varepsilon_v$), *and from the continuum spectrum* ($\varepsilon_c$).

(1) *Equilibrium composition.* The equilibrium compositions of mixtures containing the species $H_2$, H, $H^+$, $e^-$, $H^-$ and $H_2^+$ were calculated by using the methods of statistical thermodynamics. The effective lowering of the ionization potentials produced by the fields of the plasma ions was estimated[36] and found to have a small effect on the emissivities in most cases.

(2) *Emission processes.* The important emission processes may be represented by the following reactions:

1. $H_2 \rightarrow H_2 + h\nu$
   $H_2 \rightarrow H + H + h\nu$
   $H + H \rightarrow H_2 + h\nu$
2. $H \rightarrow H + h\nu$
   $H^+ + e^- \rightarrow H + h\nu$
   $H^+ + e^- \rightarrow H^+ + e^- + h\nu$
3. $H + e^- \rightarrow H^- + h\nu$
   $H + e^- \rightarrow H + e^- + h\nu$
4. $H + H^+ \rightarrow H_2^+ + h\nu$
   $H + H^+ \rightarrow H + H^+ + h\nu$

Here $e^-$ represents an electron and $h\nu$ is the emitted photon. The first group

of reactions contains processes in which $H_2$ participates, with the second and third equations in the group involving free hydrogen atoms in the lower and upper states, respectively. The second group of reactions is that corresponding to line and continuum radiation from the H atom. The third and fourth groups involve continuum radiation from the $H^-$ ion and $H_2^+$ ion, respectively.

Since the $H_2$ molecule is homonuclear, ordinary vibrational and rotational transitions are forbidden. Investigation of the other molecular emission processes shows that the "pressure-induced" spectrum gives the dominant emissivity contribution at low temperatures and high pressures. The pressure-induced spectrum consists of vibration-rotation bands and rotational lines resulting from transitions which occur during collisions when dipole moments are induced in the colliding molecules. The experimental values[37-39] for the band and line integrated intensities have been extended to higher temperatures by use of the theoretical relations of VAN KRANENDONK.[40, 41] The emissivity of the fundamental band was calculated using an average band absorption coefficient (box model). We recall that the general expression for the total emissivity $\varepsilon$ in terms of the absorption coefficient $k_\omega$ is

$$\varepsilon=\frac{1}{\sigma T^4}\int R_\omega^\circ\left[1-\exp\left(-k_\omega l\right)\right]\,\mathrm{d}\omega \tag{24}$$

where $R_\omega^\circ$ is the spectral blackbody radiancy; $l$ the mean beam length, and $\sigma$ the Stefan–Boltzmann constant. The absorption coefficient for the rotational lines was calculated from the known line contours[42] at low temperatures.

The values of the absorption coefficients for the $H^-$ ion and $H_2^+$ ion were obtained from CHANDRASEKHAR and BREEN[43] and BATES,[44] respectively. It was found that the $H_2^+$ contribution to the total emissivity is less than about 5 per cent of the $H^-$ contribution for temperatures lower than 10,000°K.

The free-free absorption coefficient for the H atom was calculated from[45]

$$\frac{k_\omega^{ff}}{p_H}=\frac{32}{3\sqrt{3}}\;\frac{\pi^2e^6R_y}{h^3c^3kT}\;\frac{\mathrm{e}^{-x_1}}{\omega^3}\left(\frac{1}{2x_1}\right)\left(1-\mathrm{e}^{-hc\omega/kT}\right)g_{ff}(\omega) \tag{25}$$

where $R_y$ is the Rydberg constant, $x_1=hcR_y/kT$, and the other symbols correspond to standard spectroscopic notation. Extrapolation of the results given in ref. 46 shows that, for the temperatures of interest in our calculation, $g_{ff}(\omega)$ may be replaced by the mean value $g_{ff}\simeq 1{\cdot}24$. Similarly, the bound–free absorption coefficient was calculated from[45]

$$\frac{k_\omega^{bf}}{p_H}=\frac{32}{3\sqrt{3}}\;\frac{\pi^2e^6R_y}{h^3c^3kT}\;\frac{\mathrm{e}^{-x_1}}{\omega^3}\left(\sum_{\omega_n<\omega}^{\infty}\frac{\mathrm{e}^{x_n}}{n^3}\;g_{bf,\,n}(\omega)\right)\left(1-\mathrm{e}^{-hc\omega/kT}\right) \tag{26}$$

where $x_n=hcR_y/kTn^2$ and $\omega_n=R_y/n^2$. The Gaunt factors $g_{bf,n}(\omega)$ vary

from about 0·90 to 1·10;[47] hence the approximation $g_{bf,n}(\omega) \simeq 1.00$ was used.

The integrated intensity of the atomic line corresponding to transitions between energy levels with quantum numbers $n$ and $n'$ was evaluated from the relation [48]

$$S_{nn'} = \frac{\pi e^2}{m_e c^2} f_{n \to n'} n^2 \left(\frac{N_H}{p_H}\right) e^{-(x_1 - x_n)} \left[1 - e^{(-hc\omega_{nn'}/kT)}\right] \qquad (27)$$

where $N_H$ is the number of hydrogen atoms per unit volume. The $f$-values $f_{n \to n'}$ were obtained from ref. 49. For a transparent gas, the total emissivity of a line is determined directly from the integrated intensity. However, for the higher temperatures and pressures of interest the gas is not transparent to the lines and, therefore, the line profiles must be considered.

At the highest pressures, the lines are primarily collision-broadened, yielding a dispersion contour for the absorption coefficient. For this case, it is well-known that the emissivity may be given in terms of the line integrated intensity $S_{n \to n'}$ and a collision half-width $b_c$.[50] Approximate relations for $b_c$ for the Balmer and Paschen lines were obtained[34] by extending the results of MARGENAU and WATSON,[51] which are applicable only to the Lyman lines. At the higher temperatures and lower pressures the hydrogen lines are primarily Stark-broadened. Using the profile in the line wings given by the Holtzmark theory, a simple expression for the emissivity of Stark-broadened lines was obtained. These results were used to calculate the emissivities of all lines except the Lyman lines.*

If the simple collision and Stark broadening theories mentioned above are used to compute the profile of the Lyman α line, the absorption coefficient far out in the wings will be appreciable because of the large integrated intensity of the Lyman α line [cf. Eq. (27)]. Even though the center of the Lyman α line is at 82,258 $cm^{-1}$, the absorption coefficient of the low wave number wing computed from the simple broadening theories is sufficiently large at low wave numbers, where the blackbody radiancy is large, to account for the major portion of the total emitted intensity of the hydrogen plasma from approximately 4000°K to 8000°K [cf. Eq. (24)]. This conclusion is, however, erroneous because the simple relations for collision and Stark broadening are not applicable very far from the line center. Accordingly, relations applicable far from the line center had to be developed. By considering the interaction potentials for close encounters between 2 H atoms and the corresponding transition probabilities for the $H_2$ molecule, the statistical theory of broadening was used to estimate the collision-broadened line profile far from the line center.[34] A similar analysis for H atom and $H^+$ ion encounters, using $H_2^+$ ion transition probabilities, yielded the Stark-broadened line profile. It was found that the absorption coefficient far out in the low wave number

* For a more accurate description of Stark-broadening, see ref. 52.

wing of the Lyman α line is thus made so small that it gives a negligibly small contribution to the emissivity. For temperatures below 10,000°K, the emissivity contribution of the Lyman lines may be neglected, except for very low pressures.*

(3) *Calculation of the total emissivity.* The total emissivity for the plasma was calculated by using for the total spectral absorption coefficient in Eq. (24) the sum of the spectral absorption coefficients for all contributing processes. When both continuum and line radiation are important, it is convenient to utilize the line emissivities directly since these can be easily calculated. For this purpose, Eq. (24) may be approximated by the expression

$$\varepsilon \simeq \varepsilon_c + \sum_i \left[ \exp\left( -k_{\omega_i}^c l \right) \right] \varepsilon_{\text{line } i} \tag{28}$$

where $\varepsilon_c$ is the continuum emissivity, $\varepsilon_{\text{line } i}$ the emissivity of the $i$th line, and $k_{\omega_i}^c$ the continuum absorption coefficient at the center of the $i$th line.

A representative emissivity calculation was made for $p_T = 100$ atm, $l =$ 30 cm, and $T$=300–10,000°K. Reference to Fig. 7 shows that the dominant emissivity contribution is provided by the pressure-induced rotational spectrum of $H_2$ at temperatures below 1200°K, by the pressure-induced fundamental band between 1200°K and 4400°K, and by the continuum radiation from 4400°K up to 10,000°K. The continuum radiation arises primarily from the $H^-$ bound-free and free-free transitions with the bound-free transitions of the H atom starting to become important at the higher temperatures. The emissivities of the atomic lines, decreased by the transmissivity of the continuum [cf. Eq. (28)], amount to less than a few per cent of the continuum emissivity.

Since the absorption coefficient for the $H^-$ ion is proportional to $p_e p_H$ and that for the H atom is proportional to $p_H$, the H atom spectrum will become more important at lower total pressures.

## REFERENCES


[1] PENNER, S. S. *Quantitative Molecular Spectroscopy and Gas Emissivities*, Addison–Wesley, Reading, Mass., 1959.

[2] CHANDRASEKHAR, S. *Radiative Transfer*, Clarendon Press, Oxford, 1950.

[3] KOURGANOFF, V. *Basic Methods in Transfer Problems*, Clarendon Press, Oxford, 1952.

[4] THOMSON, J. A. L. Gruen Applied Science Laboratories Report, Pasadena, California, April 1957.

[5] Reference 1, Chap. 13.

[6] HOTTEL, H. C. Radiant-heat transmission, Chapter IV of *Heat Transmission* by W. H. McAdams, 3rd ed., McGraw-Hill, New York, 1954.

[7] LAPP, M. Ph.D. Thesis, California Institute of Technology, Pasadena, California. A complete account of this work will be published elsewhere.


* Details concerning this analysis will be published in the near future.

[8] KECK, J., CAMM, J. and KIVEL, B. Absolute emission intensity of Schumann–Runge radiation from shock heated oxygen, *J. Chem. Phys.*, **28**, 723–724, 1958.

KECK, J., CAMM, J. and WENTINK, T. W. Jr. Radiation from hot air. Part II. Shock tube study of absolute intensities, *Ann. Phys.*, **7**, 1–38, 1959.

TREANOR, C. E. and WURSTER, W. H. Measured transition probabilities in the Schumann–Runge system of oxygen, *J. Chem. Phys.*, **32**, 758–766, 1960.

[9] OLDENBERG, O. and RIEKE, F. F. Kinetics of OH radicals as determined by their absorption spectrum. III. A quantitative test for free OH; probabilities of transition, *J. Chem. Phys.*, **6**, 439–447, 1938.

DWYER, R. J. and OLDENBERG, O. The dissociation of $H_2O$ into H+OH, *J. Chem. Phys.*, **12**, 351–361, 1944.

[10] DYNE, P. J. Uncertainties in the measurement of the oscillator strength of the ultraviolet bands of OH, *J. Chem. Phys.*, **28**, 999–1000, 1958.

[11] CARRINGTON, T. Line shape and *f* value in the $OH\,^2\Sigma^+ - {}^2\Pi$ transition, *J. Chem. Phys.*, **31**, 1243–1252, 1959.

[12] BAUER, S. H., SCHOTT, G. L. and DUFF, R. E. Kinetic Studies of hydroxyl radicals in shock waves. I. The decomposition of water between 2400° and 3200°K, *J. Chem. Phys.*, **28**, 1089–1096, 1958.

[13] Reference 1, Chap. 5.

[14] DIEKE, G. H. and CROSSWHITE, H. M. The ultraviolet bands of OH, Bumblebee Report No. 87, The Johns Hopkins University, Baltimore, Md., 1948.

[15] BRABBS, T. A., ZLATARICH, S. A. and BELLES, F. E. Limitations of the reflected-shock technique for studying fast chemical reactions, *J. Chem. Phys.*, **33**, 307–308, 1960.

[16] SKINNER, G. B. Limitations of the reflected-shock technique for studying fast chemical reactions, *J. Chem. Phys.*, **31**, 268–269, 1959.

[17] GOLDSWORTHY, F. A. The structure of a contact region, with application to the reflection of a shock from a heat-conducting wall, *J. Fluid Mech.*, **5**, 164–176, 1959.

[18] PENNER, S. S., OLFE, D. B. and JACOBS, T. A. Vibrational relaxation in cylindrical chambers containing isothermal, dilute gas mixtures, Technical Report No. 13, Contract AF 18(603)–2, California Institute of Technology, Pasadena, Calif., May 1960.

[19] BURSIAN, V. and SOROKIN, V. Anwendung der Diffusionsgleichung auf die Theorie der Kettenreaktionen, *Z. Phys. Chem.*, **12B**, 247–267, 1931.

[20] PENNER, S. S. *Chemistry Problems in Jet Propulsion*, pp. 236–238, Pergamon Press, London, 1957.

[21] RUBIN, R. J. and SHULER, K. E. Relaxation of vibrational nonequilibrium distributions. I. Collisional relaxation of a system of harmonic oscillators, *J. Chem. Phys.*, **25**, 59–67, 1956.

[22] LANDAU, L. and TELLER, E. Zur Theorie der Schalldispersion, *Phys. Z. Sowjetunion*, **10**, 34–43, 1936.

[23] Reference 1, p. 23.

[24] SHERRAT, G. and GRIFFITHS, E. The determination of the specific heat of gases at high temperature by the sound velocity method. I. Carbon Monoxide, *Proc. Roy. Soc. London*, **147A**, 292–308, 1934.

[25] BENDER, D. Ultraschallgeschwindigkeiten in Stickstoff, Stickoxyd und Kohlenoxyd zwischen 20 und 200°C, gemessen mit einem neuen Verfahren, *Ann. Phys.*, **38**, 199–214, 1940.

[26] JONES, R. C., in *Advances in Electronics*, p. 30, Academic Press, New York, 1953.

[27] LAPP, M. and PENNER, S. S. Equilibrium emissivity calculations (from spectroscopic data) for $CO_2$ at 300° and 600°K, Contract Nonr-220(03). NR 015 401, California Institute of Technology, Pasadena, Calif., June 1960.

[28] Reference 1, pp. 308–316.

[29] PLASS, G. N. Spectral emissivity of carbon dioxide from 1800–2500 $cm^{-1}$, *J. Opt. Soc. Amer.*, **49**, 821–828, 1959.

[30] FERRISO, C. C. The temperature, spectrum, and emissivity of exhaust gases from a small rocket, Report No. AZR-014, Vol. III, Convair Astronautics, San Diego, Calif., 1960.

[31] TOURIN, R. H. and HENRY, P. M. Infrared spectral emissivities and internal energy distributions of carbon dioxide and water vapor at high temperatures, AFCRC-TR-60-203, The Warner and Swasey Co., Control Instrument Division, New York, N.Y., 1959.
[32] Reference 1, pp. 317–320.
[33] Reference 1, pp. 399–400.
[34] OLFE, D. B., Ph.D. Thesis, California Institute of Technology, Pasadena, Calif., June 1960. A complete account of this work was presented by D. B. OLFE at the *Symposium of Quantitative Spectroscopy and Selected Military Applications*, California Institute of Technology, Pasadena, California, March 1960. The complete paper will be published elsewhere.
[35] MASTRUP, F. Continuous emission of hydrogen plasmas, *J. Opt. Soc. Amer.*, **50**, 32–35, 1960.
[36] UNSÖLD, A. Zur Berechnung der Zustandsummen für Atome und Ionen in einem-teilweise ionisierten Gas, *Z. Astrophys.*, **24**, 355–362, 1948.
[37] CHISHOLM, D. A. and WELSH, H. L. Induced infrared absorption in hydrogen and hydrogen-foreign gas mixtures at pressures up to 1500 atm., *Canad. J. Phys.*, **32**, 291–312, 1954.
[38] COLPA, J. P. and KETELAAR, J. A. A. The pressure-induced rotational absorption spectrum of hydrogen. I and II. *Molecular Physics*, **1**, 14–22, 343–357, 1958.
[39] KISS, Z. J., GUSH, H. P. and WELSH, H. L. The pressure-induced rotational absorption spectrum of hydrogen, *Canad. J. Phys.*, **37**, 362–376, 1959.
[40] VAN KRANENDONK, J. Induced infra-red absorption in gases. Calculation of the binary absorption coefficients of symmetrical diatomic molecules, *Physica*, **24**, 347–362, 1958.
VAN KRANENDONK, J. Theory of induced infrared- absorption, *Physica*, **23**, 825–837, 1957.
[41] VAN KRANENDONK, J. and KISS, Z. J. Theory of the pressure-induced rotational spectrum of hydrogen, *Canad. J. Phys.*, **37**, 1187–1198, 1959.
[42] KISS, Z. J. and WELSH, H. L. The pressure-induced rotational absorption spectrum of hydrogen, *Canad. J. Phys.*, **37**, 1249–1259, 1959.
[43] CHANDRASEKHAR, S. and BREEN, F. H. On the continuous absorption coefficient of the negative hydrogen ion III, *Astrophys. J.*, **104**, 430–445, 1946.
[44] BATES, D. R. Absorption of radiation by an atmosphere of H, $H^+$, and $H_2^+$– semi-classical treatment, *Roy. Astronom. Soc., Monthly Notices*, **112**, 40–44, 1952.
BATES, D. R. Rate of formation of molecules by radiative association, *Roy. Astronom. Soc., Monthly Notices*, **111**, 303–314, 1951.
[45] Reference 1, p. 170.
[46] GREENE, J. Bremsstrahlung from a Maxwellian gas, *Astrophys. J.*, **130**, 693–701, 1959.
[47] MAYER, H. Methods of opacity calculations, Los Alamos Scientific Laboratory Report LA-647, Los Alamos, New Mexico, 1947.
[48] Reference 1, p. 147.
[49] UNSÖLD, A. *Physik der Sternatmosphären*, Springer, Berlin, 1938.
[50] Reference 1, pp. 40–45.
[51] MARGENAU, H. and WATSON, W. W. Pressure effects on spectral lines, *Reviews of Modern Physics*, **8**, 22–53, 1936.
[52] MARGENAU, H. and LEWIS, M. Structure of spectral lines from plasmas, *Reviews of Modern Physics*, **31**, 569–615, 1959.